J Nanostruct 14(2): 638-645, Spring 2024

RESEARCH PAPER

Preparation and Structural Properties of In_2O_3-GO Doped PMMA-PC Blend for Antibacterial Applications

Dhay Ali Sabur *, Majeed Ali Habeeb, Ahmed Hashim

Department of Physics, College of Education for Pure Sciences, University of Babylon, Babylon, Iraq

ARTICLE INFO

Article History:
Received 07 January 2024
Accepted 19 March 2024
Published 01 April 2024

Keywords:
Antibacterial
FTIR
Nanocomposites
Nanoparticles
SEM

ABSTRACT

In this paper, films of (PMMA-PC/In_2O_3-GO) nanocomposite were prepared by casting with different concentrations of (In_2O_3-GO) NPs (0, 1.4 %, 2.8 %, 4.2 %,and 5.6 %).Various techniques including scanning electron microscopy (SEM), optical microscopy, and Fourier transform infrared spectroscopy(FTIR), were used to characterize the nanocomposites (PMMA-PC/In_2O_3-GO). Scanning electron microscopy (SEM) is used to describe the structural properties and changes in the surface morphology of nanocomposites. Optical microscopy is used to examine the homogeneity of (In_2O_3-GO) NPs within a blend (PMMA-PC). Using the vibrational modes assigned to free and hydrogen-bound hydroxyl and carbonyl groups, Fourier transforms infrared spectroscopy (FTIR) may be utilized to provide information on both blend composition and polymer-polymer interactions. Two different strains of pathogenic bacteria, Staphylococcus (G+ ve) and E. coli (G-ve) were used to investigate the effectiveness of(PMMA-PC/In_2O_3-GO). The findings showed that (PMMA-PC/In_2O_3-GO) had potent antibacterial activity and may be utilized to treat illnesses caused by one or both of these bacterial species.

How to cite this article
Sabur D., Habeeb D., Hashim A. Preparation and Structural Properties of In_2O_3-GO Doped PMMA-PC Blend for Antibacterial Applications. J Nanostruct, 2024; 14(2):638-645. DOI: 10.22052/JNS.2024.02.024

INTRODUCTION

Global challenges including environmental pollution and a lack of energy supplies have created serious problems for the human population on both a social and economic level [1]. Nanoparticles can be used in biological applications such as medication delivery, biosensors, and antimicrobial materials[2,3]. Long-term research has focused on the unique characteristics of metal nanoparticles and nanocomposites as fascinating issues from both a practical and theoretical perspective [4,5]. The most typical characteristics utilized as a standard for material certification are optical, thermal, mechanical, structural, and electrical properties [6,7]. Polymethyl methacrylate (PMMA) has been the material of choice for the production of polymeric nanocomposites due to its advantageous properties, such as perfect transparency in the visible region, high strength, good weather ability, acceptable thermal stability, compatibility with ceramics, and non-toxicity [8]. Since polycarbonate (PC), one of the most popular technical polymers, is amorphous, transparent, entirely recyclable, and derived from natural resources, it has received a lot of attention. It is capable of withstanding a variety of harsh and extreme environmental conditions. Additionally, it aids in reducing carbon impact. It has excellent

* *Corresponding Author Email: ahmed_taay@yahoo.com*

thermal and mechanical characteristics [9]. Additionally, amorphous materials offer a wide range of advantageous prospective uses related to their electrical and optical characteristics indium oxide (In_2O_3) has a wide band gap it is suitable for low-emissivity windows, photovoltaic cell, and other devices due to its high electrical conductivity and visible optical transparency. The antibacterial action of this metal oxide shows that it alters the composition of bacterial cell membranes and inhibits the function of several membrane-bound enzymes that are responsible for bacterium death[10]. Because of its two-dimensional structure, large surface area, and superior electrical properties, graphene oxide(GO) is preferred as a filler because it improves optical properties that are used in many optoelectronic applications including organic light-emitting diodes, flexible transparent electronics, organic solar cells, chemical sensors, and antibacterial[11].

MATERIALS AND METHODS

Polymethylmethacrylate (PMMA), polycarbonate (PC), indium oxide (In_2O_3), and graphene oxide (GO) were employed in this study. The casting technique was used to prepare nanocomposites films (PMMA-PC/ In_2O_3-GO). The films were prepared by dissolving 1g of the (PMMA-PC) blend with a ratio of 80/20 % in chloroform using a magnetic stirrer. The (In_2O_3-GO) NPs were introduced in the polymeric blend by (1.4%, 2.8%, 4.2%, and 5.6%). A scanning electron microscope (SEM HV:5.0 KV, Det: InBeam, MIRA3 TESCAN) was used to test the

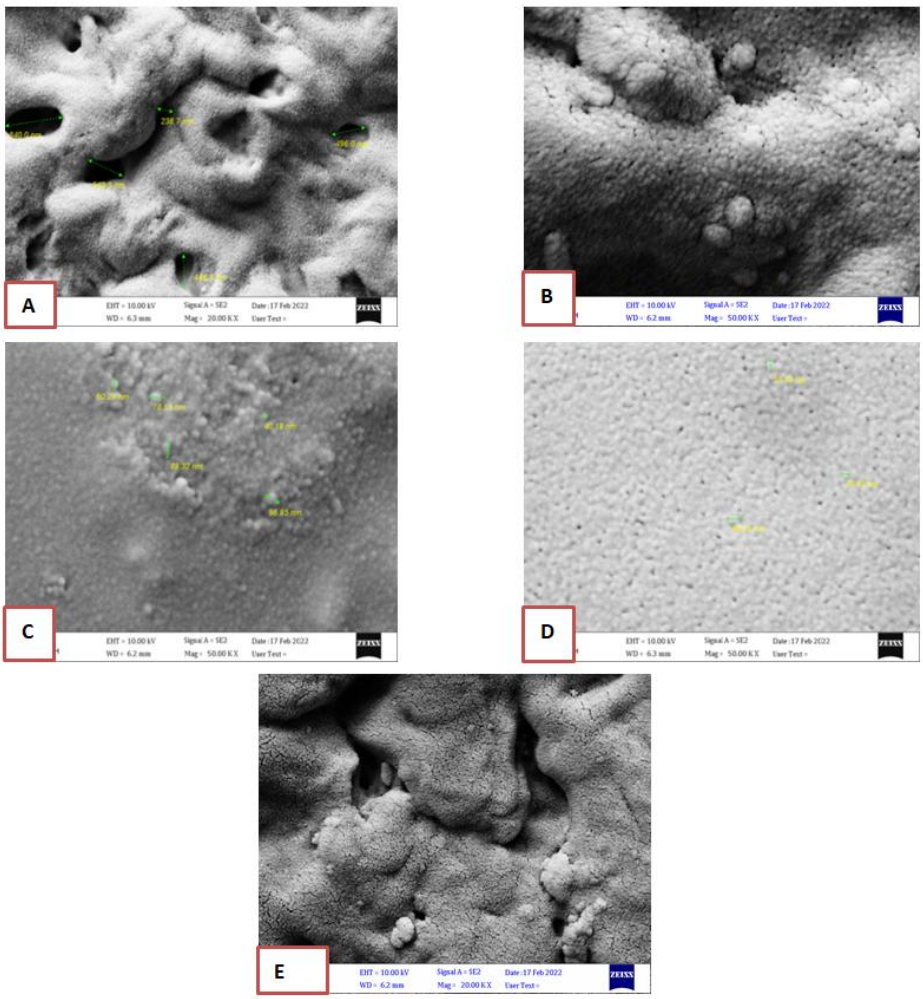

Fig. 1. SEM images for (PMMA-PC/In_2O_3-GO) Nanocomposites: (A) for pure (B) for 1.4 wt.% In_2O_3-GO NPs (C) for 2.8 wt.% In_2O_3-GO NPs (D) for 4.2wt.% In_2O_3-GO NPs (E) for 5.6 wt.% In_2O_3-GO NPs

surface morphology of (PMMA-PC/In_2O_3-GO) nanocomposites. In this study, FTIR spectra were recorded by FTIR (Bruker company, German origin, type vertex -70) at the considered wavenumber range is (4000-500) cm^{-1}. For antibacterial activity, using the disc diffusion technique the antibacterial activity of the investigated samples of (PMMA-PC/In_2O_3-GO) nanocomposites was assessed. Gram-positive (Staphylococc aureus) and gram-negative (Escherichia coli) bacteria were both cultivated on Muller-Hinton agar a. The disks of the (PMMA-PC/In_2O_3-GO) nanocomposites were positioned on top of the medium and incubated for 24 hours at 37°C. Measurements were made on the inhibition zone diameter.

RESULTS AND DISCUSSION

Fig. 1 illustrates how scanning electron microscopy is used to identify phase separations and interfaces in order to examine the compatibility between different polymer and nanomaterial components. All figures display incredibly fine three-dimensional representations at extreme magnifications. [12]. The surface structure of the (PMMA-PC) blend without and with the presence of nanoparticles can be imaged through (SEM) with high clarity. The surface morphology of a film made of a PMMA-PC blend of polymers is shown in (SEM) images before and after the addition of a concentration of (In_2O_3-GO) nanoparticles. The films show a uniform distribution of grains

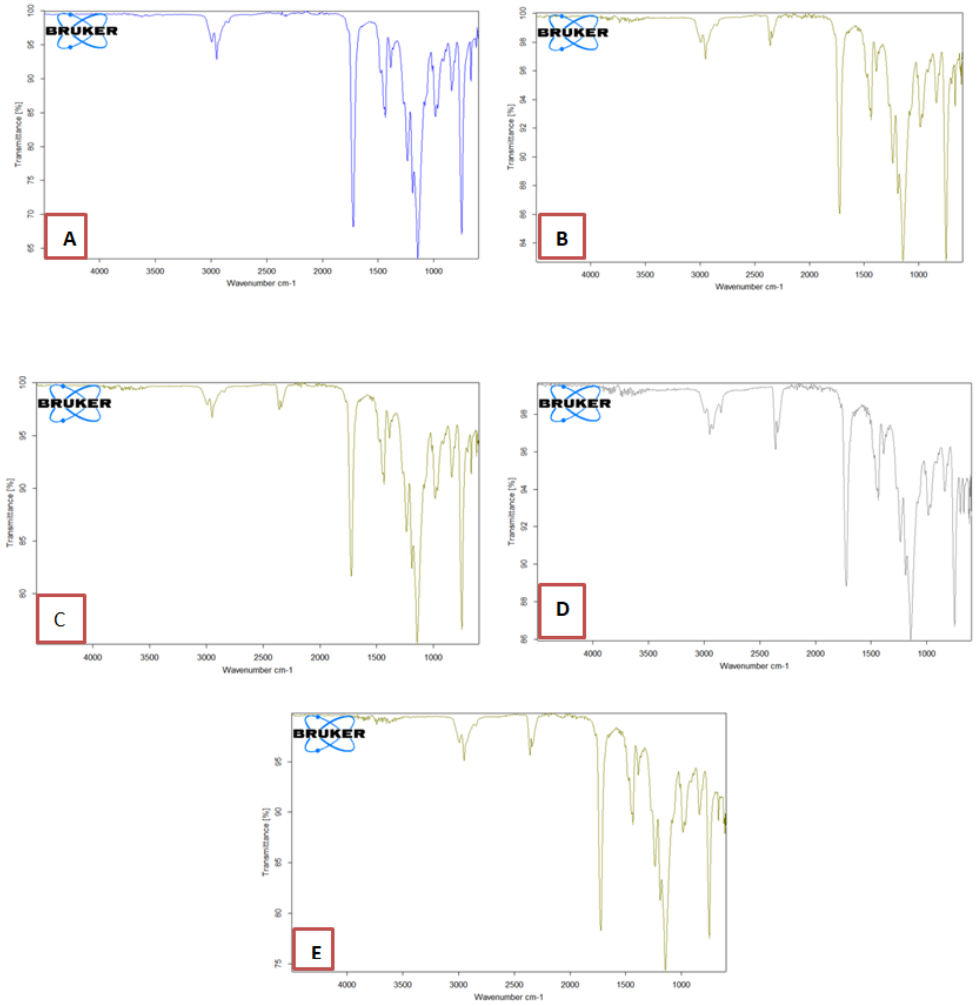

Fig. 2. FTIR spectra for (PC-PMMA-In_2O_3-GO) NPs (A)for (PMMA-PC) blend (B) for 1.4wt% (In_2O_3-GO) NPs ,(C) for 2.8wt% (In_2O_3-GO) NPs ,(D)for 4.2wt% (In_2O_3-GO) NPs , (E) for 5.6wt% (In_2O_3-GO) NPs.

at the surface, while the surface morphology of the (PMMA-PC/In_2O_3-GO) nanocomposites films exhibits a large number of aggregates or pieces of randomly dispersed nanoparticles. the micrographs show that the films are dense, smooth, and have a compact structure[13].The results indicate that the nanoparticles tended to form aggregates and good dispersed (PMMA-PC/In_2O_3-GO). Also Fig. 1 observed that the (In_2O_3-GO) nanoparticles are randomly distributed in the (PMMA-PC) polymers films and concluded that small agglomerations is formed in this films. When adding the concentrations nanoparticles (In_2O_3-GO) to (PMMA-PC) polymers form a continuous network inside the polymers with more magnifications resolutions for (PMMA-PC/In_2O_3-GO) polymers nanocomposites films and (PMMA-PC/In_2O_3-GO) Network has paths where charge carriers are allowed to pass through the paths that have low electrical resistance. These results are in agreement with results. Also with increasing the concentrations of nanoparticles, the surfaces area for all films are increasing for this reason increasing the absorbance for all films [14].

Fig. 2 shows Three regions are included in the FTIR spectra of the (PMMA-PC)blend. The first one

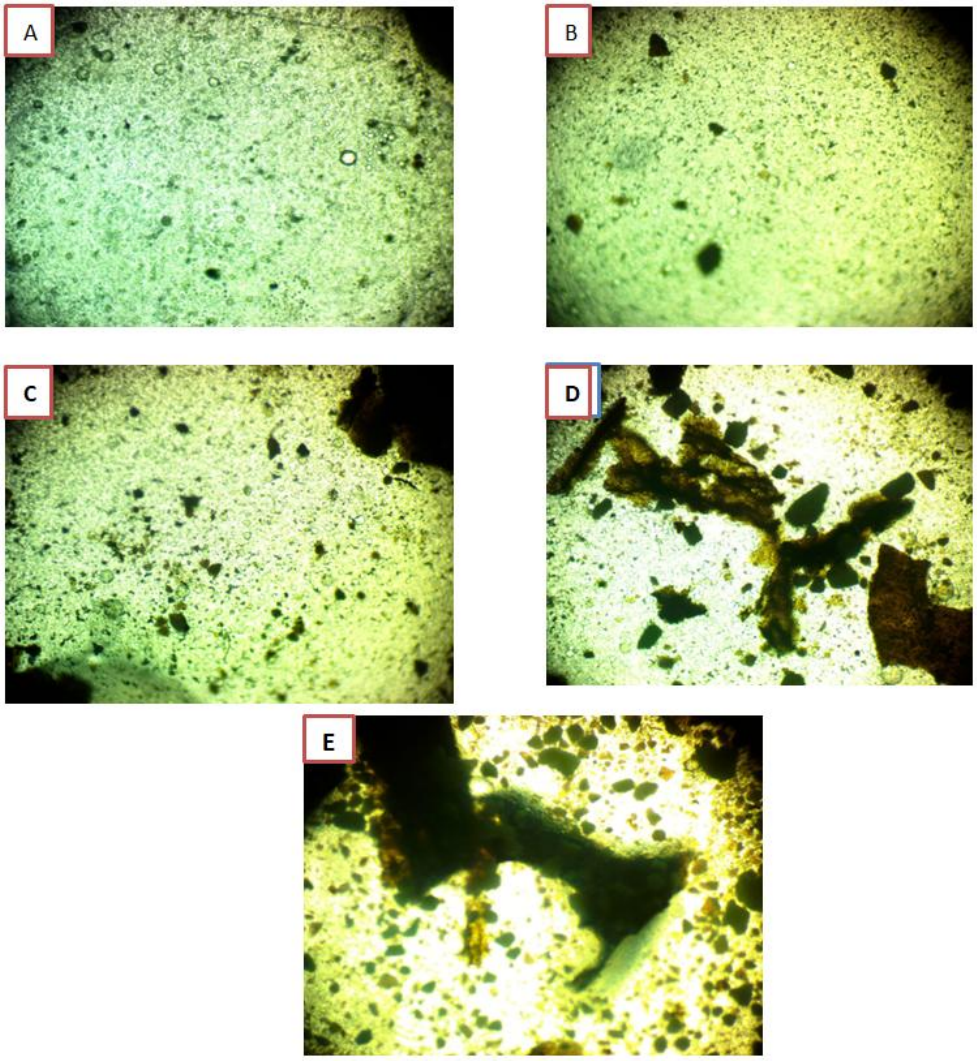

Fig. 3. Photomicrographs for (PMMA-PC/In_2O_3-GO) nanocomposites (A)for (PMMA-PC) blend (B) for 1.4wt% In_2O_3-GO nanoparticles,(C) for 2.8wt% In_2O_3-GO nanoparticles,(D) for 4.2wt% In_2O_3-GO nanoparticles, (E) for 5.6wt% In_2O_3-GO nanoparticles

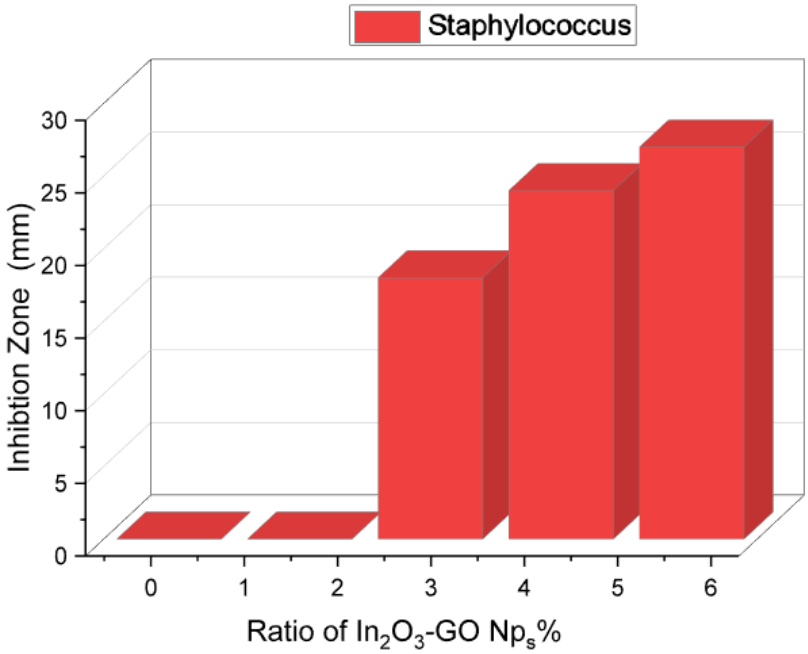

Fig. 4. Variation of inhibition zone diameter with (In_2O_3-GO)NPs concentrations against Staphylococcus for (PMMA-PC/ In_2O_3-GO) nanocomposites.

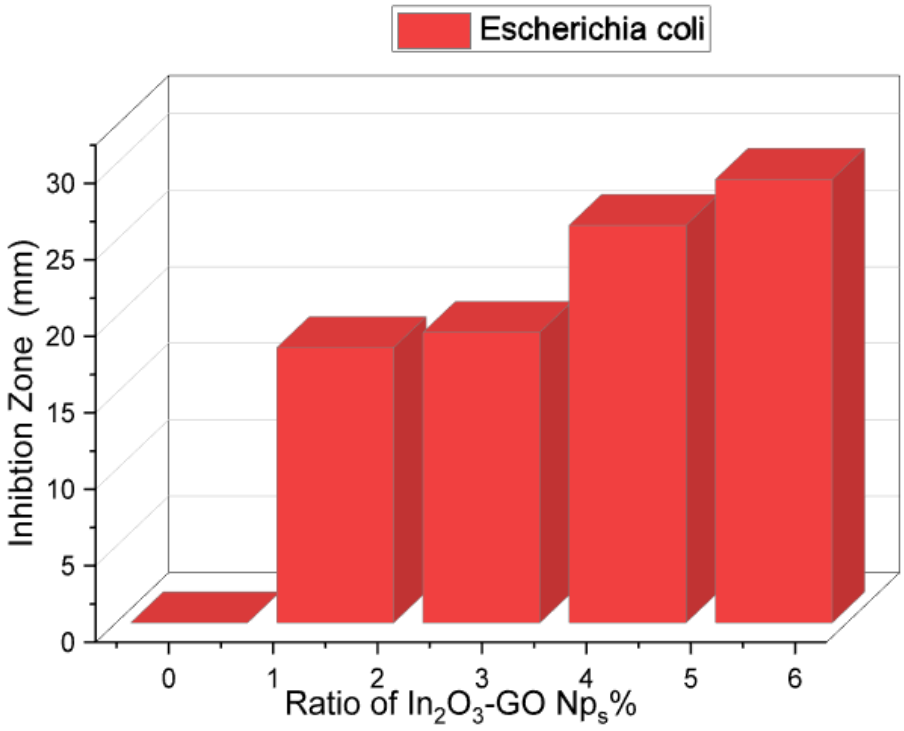

Fig. 5. Variation of inhibition zone diameter with (In_2O_3-GO)NPs concentrations against Escherichia coli for (PMMA-PC/ In_2O_3-GO) nanocomposites.

is a broad, absorption peak band that arises at 3285 cm^{-1} and is connected to the stretching of the O-H hydroxyl group, which is a particularly strong bond because it appears at a high wavelength range. The second zone, which has slightly stronger bonding, is visible between 2859 and 2882 cm^{-1} in wavelength[15]. The peaks that are visible in this area indicate that C-H has extended into the PMMA-PC structure. The third area, which is related to C-O stretching, is characterized by weak bonding and may be seen at low wavelengths between 1050 and 1350 cm^{-1}. Fig. 2 shows the FT-IR of composite films made of (PMMA-PC/In_2O_3-GO) C-H, NH_2, and C=O are the three new bonds. A prominent, wide-range absorption band with the first region of roughly 2700-3600 cm^{-1} is where NH_2 stretching is seen. In the second area, which is likewise a part of the PMMA-PC structure and is in the range of 2859-2882 cm^{-1}, C-H stretching is produced. At the third zone of weak absorption bands and low wavelengths of around 1730-1735 cm^{-1}, the C=O and amidic bonds are freshly created .The chemical reaction between nanopowder and the polymeric blend does not emerge from FT-IR, indicating that there was just physical blending since the bonds that belong to nanocomposite do not appear and there are no new peaks in the IR spectrum [17].

Fig. (A, B, C, D, and E) show microscopic images of a (PMMA-PC) blend with varying weight percentages of (In_2O_3-GO) nanoparticles. Fig. 2 shows the surface structure of the pure polymeric blend (PMMA-PC) was homogeneous and devoid of any agglomeration and porosity Due to the homogenous mixing of PMMA and PC [18]. The surface structure of the PMMA-PC blend with 1.4 weight percent (In_2O_3-GO) nanoparticles is depicted Fig. 2. B. Inhomogeneous mixing between the PMMA-PC blend and (In_2O_3-GO) nanoparticles may be the cause of the very minute dark patches that have spread across the polymer host material following the addition of nanoparticles, Agglomeration size grew increasingly as the number of nanoparticles increased. weight percent as observed from Fig. 2.C,2.D.and 2.E, also when In_2O_3 and GO nanoparticles reach to higher concentration the fillers materials form an uninterrupted network inside the polymer blend. This constitute paths inside the nanocomposites of charge carriers, this system can allow charge carriers to pass through the paths [19]. Figs. 4 and 5 illustrate the antibacterial activity of (PMMA-PC/In_2O_3-GO) nanocomposites samples when tested against gram-negative (Staphylococcus) and gram-positive (Escherichia coli) bacteria, respectively. The inhibition zone grows as the concentration of (In_2O_3-GO) nanoparticles increases[20]. Reactive oxygen species (ROS), which are produced at various concentrations of (In_2O_3-GO) nanoparticles, may be the cause of the antibacterial activity of (PMMA-PC/In_2O_3-GO) nanocomposites. It's possible that membrane proteins and hydrogen

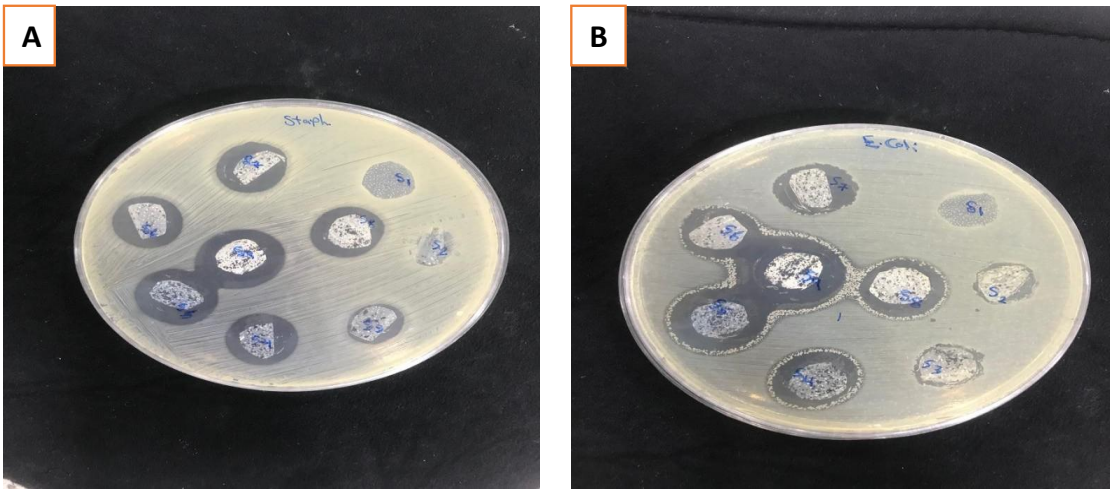

Fig. 6. (Antibacterial activity of (PMMA -PC/In_2O_3- GO) nanocomposite. Zone of inhibition of (PMMA -PC/In_2O_3- GO) nanocomposite against A: Staphylococcus: , B: Escherichia coli.

peroxide's chemical interaction is what gives nanocomposites their antibacterial properties. Bacteria are killed when the hydrogen peroxide generated reaches their cell membranes. The other conceivable mechanism of action is that the electromagnetic attraction between the nanoparticles and the microorganisms is caused by the positive charges carried by the (In_2O_3-GO) nanoparticles in nanocomposites and the negative charges held by the bacteria. The germs rapidly perish when the attraction is created because they oxidize. With an increase in the weight percentages of (In_2O_3-GO) nanoparticles, the findings showed that (PMMA- PC/In_2O_3-GO) films had a good antibacterial activity [21,22,23]. In Fig. 6 the antibacterial mechanisms of (In_2O_3-GO) Nps effect on bacteria are briefly explained The (In_2O_3-GO) Nps attachment to the bacterial cell wall induced a buildup of the envelope protein precursors, which resulted in the rapid loss of proton motive force. Because phosphate groups and sulfur are found in the base of DNA, (In_2O_3-GO) can interact with it and impact how well DNA replicates. Furthermore, (In_2O_3-GO) demonstrates instability in the rupturing of the plasma membrane and outer membrane, resulting in ATP depletion. Additionally, (In_2O_3-GO) can enter the cell membrane by adhering to the surface and preventing cell respiration. The cations (In_2O_3-GO) bind with thiol groups of bacterial proteins and leading to cell death [24].

CONCLUSION

This work includes the synthesis of (PMMA -PC/In_2O_3- GO) nanocomposite and studying the structure, and activity of (PMMA- PC/In_2O_3-GO) nanocomposites as antibacterial. The scanning electronic microscope SEM shows that aggregates or chunks on the surface that are homogenous and coherent. The FTIR shown the surface structure of the pure polymeric blend (PMMA-PC) is homogeneous and free of any agglomeration and porosity, A decrease in the intensity of peaks in the FT-IR spectrum confirms that after addition, the number of (PMMA-PC) chains increases in the structure of the films, and we draw the conclusion that the polymers after additive may have formed chains networks of polymers nanocomposites. These effects appeared in optical and electrical properties. (PMMA- PC/In_2O_3-GO) nanocomposites that have been synthesized also have effective antibacterial properties against two separate pathogenic bacterial strains. Therefore, the food, drug, and beauty industries may all benefit from this. According to the current study, biosynthesized nanoparticles can exhibit strong antibacterial activity, which opens up a wide range of options for the development of antibiotics and other medications to combat different pathogenic bacterial strains.

CONFLICT OF INTEREST

The authors declare that there is no conflict of interests regarding the publication of this manuscript.

REFERENCES

1. Dhillon A, Kumar D. Recent advances and perspectives in polymer-based nanomaterials for Cr(VI) removal. New Polymer Nanocomposites for Environmental Remediation: Elsevier; 2018. p. 29-46.
2. Rashid FL, Redha ZAA, Habeeb LJ. Thermal Energy Storage Systems: Design and Applications: Book Publisher International (a part of SCIENCEDOMAIN International); 2021 2021/02/13.
3. Hassan ES, Qader KY, Hadi EH, Chiad SS, Habubi NF, Abass KH. Sensitivity of Nanostructured Mn-Doped Cobalt Oxide Films for Gas Sensor Application. Nano Biomed Eng. 2020;12(3).
4. Srivastava S, Haridas M, Basu JK. Optical properties of polymer nanocomposites. Bull Mater Sci. 2008;31(3):213-217.
5. Abdullah OG, Hanna RR, Salman YAK. Structural, optical, and electrical characterization of chitosan: methylcellulose polymer blends based film. Journal of Materials Science: Materials in Electronics. 2017;28(14):10283-10294.
6. Etchegoin PG, Le Ru EC, Meyer M. Erratum: "An analytic model for the optical properties of gold" [J. Chem. Phys. 125, 164705 (2006)]. The Journal of Chemical Physics. 2007;127(18).
7. Jeon I-Y, Baek J-B. Nanocomposites Derived from Polymers and Inorganic Nanoparticles. Materials. 2010;3(6):3654-3674.
8. Abdelamir AI, Al-Bermany E, Sh Hashim F. Enhance the Optical Properties of the Synthesis PEG/Graphene- Based Nanocomposite films using GO nanosheets. Journal of Physics: Conference Series. 2019;1294(2):022029.
9. Kadhim MA, Al-Bermany E. Structural and DC-electrical properties of novel PMMA-PVA nanocomposites reinforced with graphene nanosheets. IOP Conference Series: Materials Science and Engineering. 2021;1067(1):012120.
10. Agarwal S, Saraswat YK, Saraswat VK. Synthesis and Thermal Characterization of Titanium-Dioxide Filled Polycarbonate/ Polystyrene Blend Nanocomposites. Macromolecular Symposia. 2015;357(1):70-73.
11. Lawal AT. Recent progress in graphene based polymer nanocomposites. Cogent Chemistry. 2020;6(1):1833476.
12. Aziz SB, Abidin ZHZ. Electrical and morphological analysis of chitosan:AgTf solid electrolyte. Materials Chemistry and Physics. 2014;144(3):280-286.
13. Aziz SB, Abdullah RM. Crystalline and amorphous phase identification from the tanδ relaxation peaks and impedance plots in polymer blend electrolytes based on

[CS:AgNt]x:PEO(x-1) (10 ≤ x ≤ 50). Electrochimica Acta. 2018;285:30-46.
14. Hashim A, Hadi Q. Novel of (Niobium Carbide/Polymer Blend) Nanocomposites: Fabrication and Characterization for Pressure Sensors. Sensor Lett. 2017;15(11):951-953.
15. Nearly Monodisperse Cu_2O and CuO Nanospheres: Preparation and Applications for Sensitive Gas Sensors. American Chemical Society (ACS).
16. Pendashteh A, Mousavi MF, Rahmanifar MS. Fabrication of anchored copper oxide nanoparticles on graphene oxide nanosheets via an electrostatic coprecipitation and its application as supercapacitor. Electrochimica Acta. 2013;88:347-357.
17. Vimala K, Yallapu MM, Varaprasad K, Reddy NN, Ravindra S, Naidu NS, et al. Fabrication of Curcumin Encapsulated Chitosan-PVA Silver Nanocomposite Films for Improved Antimicrobial Activity. J Biomater Nanobiotechnol. 2011;02(01):55-64.
18. Mihai M, Ton-That M-T. Novel polylactide/triticale straw biocomposites: Processing, formulation, and properties. Polymer Engineering & Science. 2013;54(2):446-458.
19. Uddin MJ, Chaudhuri B, Pramanik K, Middya TR, Chaudhuri B. Black tea leaf extract derived Ag nanoparticle-PVA composite film: Structural and dielectric properties. Materials Science and Engineering: B. 2012;177(20):1741-1747.
20. Prabhu YT, Rao KV, Kumari BS, Kumar VSS, Pavani T. Synthesis of Fe_3O_4 nanoparticles and its antibacterial application. International Nano Letters. 2015;5(2):85-92.
21. Xiufang B, Nan N, Xiaoqiong W, Mingyuan L, Yage X, Zhenming C. Author response for "Comparison of high-pressure processing, ultrasound and heat treatments on the qualities of a gallic acid copigmented blueberry–grape–pineapple–cantaloupe juice blend". Wiley; 2022.
22. Das G, Kalita RD, Gogoi P, Buragohain AK, Karak N. Antibacterial activities of copper nanoparticle-decorated organically modified montmorillonite/epoxy nanocomposites. Applied Clay Science. 2014;90:18-26.
23. Tong G, Yulong M, Peng G, Zirong X. Antibacterial effects of the Cu(II)-exchanged montmorillonite on Escherichia coli K88 and Salmonella choleraesuis. Vet Microbiol. 2005;105(2):113-122.
24. Hu C-H, Xia M-S. Adsorption and antibacterial effect of copper-exchanged montmorillonite on Escherichia coli K88. Applied Clay Science. 2006;31(3-4):180-184.